Available online at www.sciencedirect.com
ScienceDirect
Journal of Power Sources 163 (2006) 76–81
JOURNAL OF POWER SOURCES
www.elsevier.com/locate/jpowsour

Short communication

PEM fuel cell electrocatalyst durability measurements

Rod L. Borup [a,*], John R. Davey [a], Fernando H. Garzon [a], David L Wood [a,b], Michael A. Inbody [a]

[a] *Los Alamos National Laboratory, MST-11, Electronic and Electrochemical Materials and Devices Group, MS J579, P.O. Box 1663, Los Alamos, New Mexico 87545, USA*
[b] *Department of Chemical and Nuclear Engineering, University of New Mexico, Albuquerque, USA*

Received 15 July 2005; received in revised form 15 February 2006; accepted 6 March 2006
Available online 27 April 2006

Abstract

Electrode material durability is an important factor in limiting the commercialization of polymer electrolyte membrane fuel cells (PEMFCs). PEMFCs typically use carbon supported nanometer sized Pt and/or Pt alloy catalysts for both anode and cathode. Electrocatalyst surface area loss is due to the growth of platinum particles. Particle size growth is accelerated by potential cycling whether due to artificial potential cycling or by cycling during fuel cell operation. Catalysts were analyzed by X-ray diffraction (XRD) to determine the degree of electrocatalyst sintering. Cathode Pt particle size growth is a function of temperature, test length and potential. The largest increase in cathode Pt particle size was observed during potential cycling experiments and increased with increasing potential. During single cell durability testing, the cathode catalyst particle size grew from about 1.9 to 3.5 nm during the drive cycle experiments over 1200 h of testing. This extent of growth was greater than that observed during steady-state testing, where the particles grew to 2.6 nm at 900 h and 3.1 nm over 3500 h. During cycling measurements, catalyst coarsening rates exhibited a linear increase with temperature. Low relative humidity decreased platinum particle growth, but substantially increased carbon loss. Carbon corrosion of the electrode catalyst layer was found to increase with increasing potential and decreasing humidity.

Keywords: PEM fuel cell durability; Platinum electrocatalyst; Electrochemically active surface area; Catalyst aging; Electrochemical potential cycling; Fuel cell drive cycle

1. Introduction

The durability of polymer electrolyte membrane (PEM) fuel cells is a major barrier to the commercialization of these systems for stationary and transportation power applications. Commercial viability depends on improving the durability of the fuel cell components. Durability is difficult to quantify and improve primarily because of the quantity and duration (i.e., up to several thousand hours or more) of testing required. To improve fuel cell durability the individual components need to be well-characterized to determine and quantify degradation mechanisms that occur.

Electrode durability is an important factor limiting the commercialization of polymer electrolyte membrane fuel cells (PEMFCs). PEMFCs typically use carbon supported nanometer sized Pt and/or Pt alloy catalysts for both anode and cathode. Earlier studies [1,2] have shown that PEMFCs operating under constant potential for thousands of hours gradually lose catalytic active surface area by nano-particle grain growth. Recent testing indicates that potential cycling accelerates the rate of surface area loss [3,4]. In this investigation, we examine the durability of Pt electrocatalysts, and the effect that fuel cell operating conditions have on the electrocatalyst durability by measuring the loss of electrochemically active surface area and changes to electrocatalyst particle size occurring during various types of testing.

2. Experimental

The LANL decal method was used to prepare all MEAs (membrane-electrode-assemblies) for this study [5,6]; the membrane for all MEAs was N112 (Nafion). PEM fuel cell durability testing was performed on single cells with active areas of 5 and 50 cm^2. Tests were conducted with steady-state conditions (both constant voltage and constant current) and with dynamic

* Corresponding author. Tel.: +1 505 667 2823; fax: +1 505 665 9507.
E-mail address: Borup@lanl.gov (R.L. Borup).

0378-7753/$ – see front matter © 2006 Elsevier B.V. All rights reserved.
doi:10.1016/j.jpowsour.2006.03.009

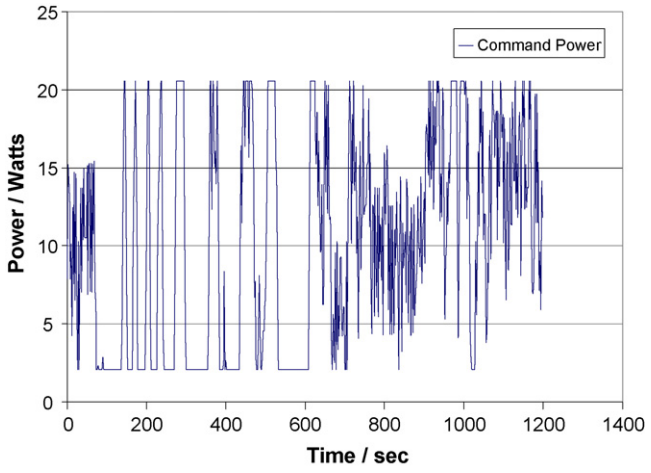

Fig. 1. Fuel cell test drive cycle based on a fuel cell hybrid vehicle operating on the US06 drive cycle.

conditions using simulated vehicle drive cycles. The dynamic conditions simulate the US06 drive cycle. Cell voltage was computer-controlled to a 20 min voltage drive cycle derived from the measured single cell polarization curve and a fuel cell power drive cycle. Anode and cathode flow rates, humidification and temperature were held constant while the voltage was varied. Fig. 1 shows the commanded power for a single cell derived from simulating a hybrid fuel cell vehicle operating on the US06 drive cycle [7]. Measurements of polarization curves, membrane resistance, hydrogen cross-over and electrochemical surface area are made in situ periodically during testing to characterize those fundamental properties changing as a function of time. Scanning electron microscopy (SEM/EDS), X-ray fluorescence (XRF), X-ray diffraction (XRD), and transmission electron microscopy (TEM) were used to characterize changes in the membrane and electrocatalyst after the durability test.

A potential sweep method was applied to single cells to investigate the effect of potential cycling on electrocatalyst growth, and its use as an accelerated testing technique. During potential sweeping, the anode was exposed to hydrogen while the cathode was exposed to nitrogen. The cathode potential was swept linearly with time from an initial voltage (usually 0.1 V) to an upper limit voltage, which was varied from 0.8 to 1.5 to observe the potential effect. The cycling was done in increments of 300 cycles. Operating conditions were: counter/reference electrode gas: hydrogen working electrode gas: nitrogen, $P_{\text{counter/reference}} = 20$ psig, $P_{\text{working}} = 30$ psig, ref. electrode, hydrogen @ 20 sccm (cm^2-active area)$^{-1}$. Working electrode, nitrogen @ 100 sccm (cm^2-active area)$^{-1}$. Other conditions were varied to examine the individual conditions on electrocatalyst growth, with a set of base conditions for comparison as: voltage range: 0.11–0.96 V, scan rate 10 mV s^{-1}, $\text{RH}_{\text{Nitrogen}} = 105\,^{\circ}\text{C}$ (226%), $\text{RH}_{\text{Hydrogen}} = 80\,^{\circ}\text{C}$ (100%) and $\text{Temp}_{\text{cell}} = 80\,^{\circ}\text{C}$. These variables were varied from the base conditions to examine their effect on catalyst stability.

Polarization curves were performed prior to cycling and after each set of 300 CV cycles to establish initial baseline performance and subsequent performance changes. The polarization curves were collected using standard conditions: cell temperature = 80 °C; anode: H_2 @ 32 sccm (cm^2-active area)$^{-1}$, humidifier temperature = 105 °C, 30 psig; cathode: air @ 100 sccm (cm^2-active area)$^{-1}$, humidifier temperature = 80 °C, 30 psig. Characterization cyclic voltammograms (CV) were performed initially and after each set of 300 CV cycles to quantify the active catalyst surface area. The characterization CVs were run under the following standard conditions: scanning from 0.11 to 1.0 V at 100 mV s^{-1}; cell temperature = 80 °C; ref. electrode: H_2 @ 20 sccm (cm^2-active area)$^{-1}$, humidifier temperature = 105 °C, 20 psig; working N_2 @ 100 sccm (cm^2-active area)$^{-1}$, humidifier temperature = 80 °C, 30 psig.

Post-cycling experiments, XRD analyses were performed to quantify changes in catalyst particle size. Catalyst was removed from the MEA by scraping the catalyst layer with a knife edge, removing as much of the catalyst layer as possible (approximately 90%). After scraping, XRDs of the catalyst powder were performed and fitted to determine volume weighted average particle size and particle size distribution. XRDs were performed in a Siemens/Bruker D5000 unit with a graphite diffracted beam monochromator Kα1 and Kα2. Shadow (MDI) software was used for whole profile fitting and data analysis. The X-ray scattering of the Pt catalyst, carbon support and residual recast NAFION ionomer were simultaneously convoluted and a least squares minimization fitting routine was used to obtain the best fit for catalyst lattice parameter, concentration and particle size.

Particle size distributions were obtained by Warren-Averbach analysis (WINFIT) of the Pt catalyst diffraction peak profiles. The (1 1 1), (2 0 0), (2 2 0), (3 1 1) and (2 2 2) Pt reflections where fit using Pearson VII functions and Fourier transformed to obtain particle size distributions.

3. Results

The electrochemical active surface area of Pt has been measured to decrease over time during operation [1,2,4], although X-ray fluorescence analyses showed no net loss of Pt [4]. The loss of surface area is accelerated when the testing includes power cycling [4]. To identify the role that the electrochemical change in potential plays in loss of electrocatalytic surface area, potential sweeping of an MEA was conducted. This examined the operating conditions and their contribution to loss of electrochemical surface area. Measured electrochemical surface areas during 1500 cycles to 0.75, 0.96, 1.0 and 1.2 V are shown in Fig. 2. A decrease in the electrocatalytic surface area for each measurement (every 300 cycles) was observed; the increase in the rate of surface area loss was observed to be a function of increasing cycling potential.

To help identify the cause of Pt surface area loss, XRD was used to measure the particle size of the electrocatalyst. The XRD patterns for three Pt electrocatalysts are shown in Fig. 3: (a) fresh Pt catalyst, (b) anode catalyst and (c) cathode catalyst after testing for 3500 h at 0.6 V. The electrocatalysts after testing show a narrowing of the diffraction peaks, which is an indication of larger particles compared with the fresh catalyst particles. Peak broadening was due to particle size broadening only no strain broadening was observed in Hall Willamson plotting of the data.

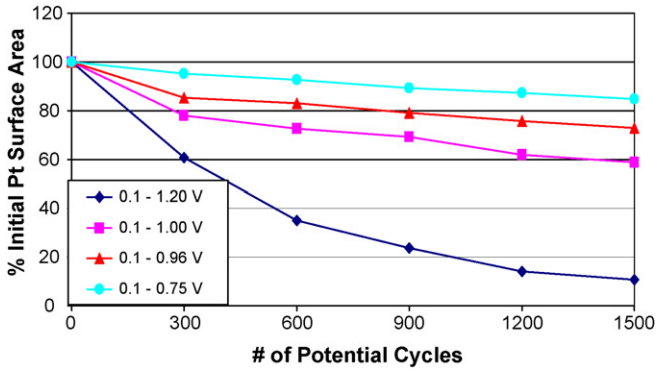

Fig. 2. Potential effect on catalyst surface area loss.

In the absence of strain, diffraction peaks breadths are broadened by particle size as in Eq. (1):

$$L_{\text{vol}} = \frac{K\lambda}{\beta \cos\theta(\text{radians})} \quad (1)$$

where K is a constant approximately equal to 1, λ is the X-ray wavelength and β is the integral breadth of the diffraction peak. This growth in electrocatalyst particle size can be correlated to the loss in electrocatalytic surface area by plotting the measured catalyst surface area versus measured Pt particle size. This is shown in Fig. 4 for catalysts that were potentially cycled to 0.75, 0.96, 1.0 and 1.2 V. The platinum particle size increases with decreasing catalytic surface area, thus the measured Pt particle size correlates with the measured electrochemically active surface area, indicating that the loss of surface area is directly due to the growth of Pt particles, as opposed to loss of Pt from the sample.

Cathode catalyst particle size increased in all of the experiments with particle growth depending on temperature, test length, and sweep potential. Growth of cathode catalyst particle size was greatest in the potential sweeping experiments and increased with increasing potential. During single cell fuel cell durability testing, the cathode catalyst particle size grew from 1.9 to 3.5 nm during the drive cycle experiments. This was a greater rate of particle growth than that observed during steady-state testing, where the particles grew to 2.6 nm at 900 h and 3.1 nm

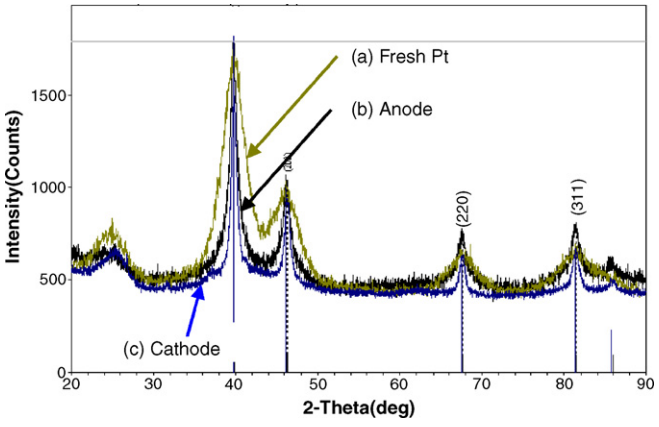

Fig. 3. X-ray diffraction patterns for (a) fresh Pt catalyst, (b) anode Pt catalyst and (c) cathode Pt catalyst after fuel cell testing at 0.60 V for 3500 h.

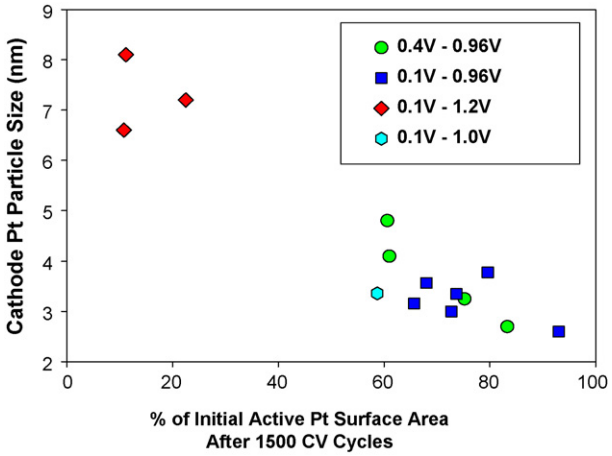

Fig. 4. Particle size as determined by XRD and measured electrochemical active surface area for various potential cycling experiments. Cell 80 °C, H_2 226% RH, Air 100% RH.

at 3500 h. During cycling measurements, the particle size grew depending upon potential (Fig. 4). The anode catalyst size was nearly uniform at about 2 nm for all experiments.

The potential cycling results show that the catalyst particle size increases with increasing potential. However, due to utilizing a linear sweep rate, this also increased the amount time at the high potentials. To identify whether time at high potential or the number of cycles was the main contribution to the particle size growth, cycling was conducted at different sweep rates, 10 and 50 mV s^{-1}. This comparison is shown in Fig. 5. The electrochemical surface area is plotted for the two sweep rates as a function of time over 0.90 V. As seen in the comparison, the number of cycles is the dominant effect in the loss of platinum surface area, time at high potential has a secondary effect.

The effect of operating temperature was also examined during potential cycling, and is shown in Fig. 6. An increase in operating temperature causes the rate of particle size growth to increase more rapidly. The relative humidity was also observed to have an effect on the growth of platinum particles. The lower the relative humidity, the less the platinum particles were observed to grow

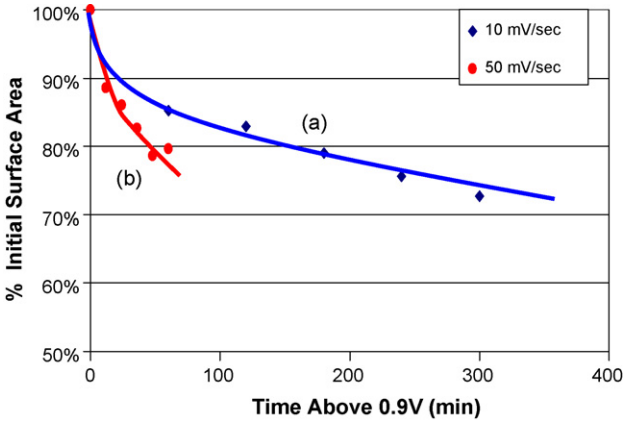

Fig. 5. Electrocatalyst surface area during cycling experiments comparing scan rates of (a) 10 mV s^{-1} and (b) 50 mV s^{-1}. Plotted as a function of time above 0.9 V. Cycling conditions: 0.4 mg cm^{-2}, 0.1–0.96 V cell 80 °C, $T_{\text{anode humidifier}}$ = 105 °C, $T_{\text{cathode humidifier}}$ = 80 °C.

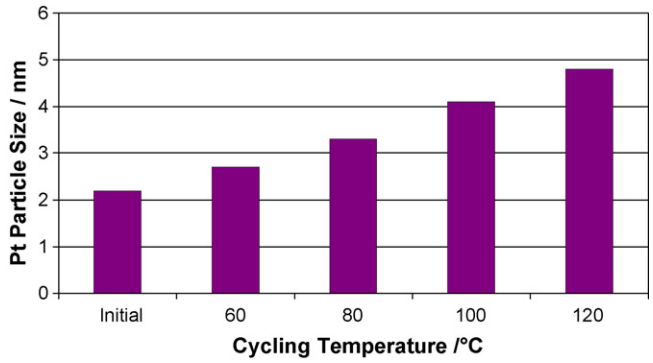

Fig. 6. Platinum particle size after cycling from 0.1 to 0.96 V as a function of operating cell temperature.

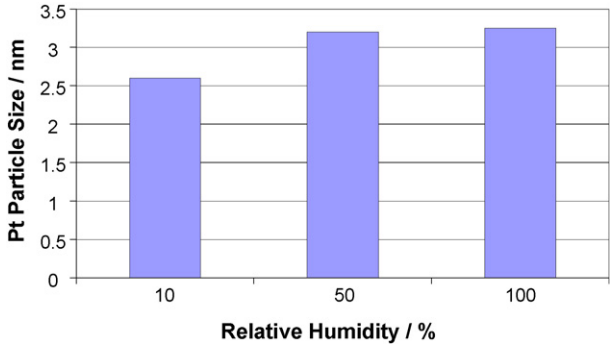

Fig. 7. Platinum particle size after cycling from 0.1 to 0.96 V as a function of operating cell relative humidity.

during the course of potential cycling. This is shown in Fig. 7. The effect of catalyst loading was also examined, varying the loading from 0.40 to 0.2 mg cm^{-2} of Pt. The change in loading did not show a difference in platinum particle size growth.

The corrosion of the catalyst support, carbon, is also an issue with electrocatalyst durability. The relative corrosion of carbon during potential cycling was measured by comparing the XRD signals of Pt and carbon (both pre- and post-cycling). The same conditions were examined as for platinum particle sintering, including sweep rate, potential, humidity, catalyst loading and temperature. The effect of potential on carbon corrosion during the cycling is shown in Fig. 8. As the potential increases,

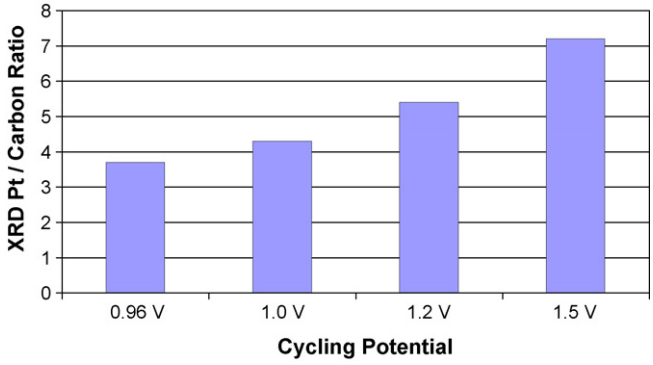

Fig. 8. The ratio of Pt to carbon XRD signals after cycling measurements for potentials of 0.96, 1.0, 1.2 and 1.5 V (after 1500 cycles, except after only 600 cycles for the cycling to 1.5 V).

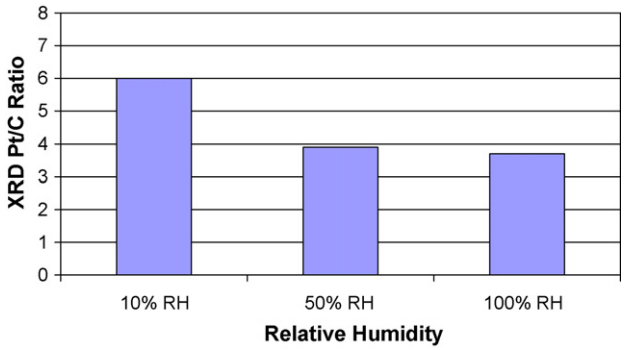

Fig. 9. The ratio of Pt to carbon XRD signals after cycling measurements at relative humidity's of 10, 50 and 100%.

the relative content of carbon decreases, indicating significant carbon corrosion. Similarly, at lower relative humidity, carbon corrosion is more prevalent than at high humidity (see Fig. 9). Temperature, sweep rate and catalyst loading did not show an effect on carbon corrosion.

4. Discussion and analysis

The loss of electrochemical active surface area appears primarily due to increasing platinum particle size. Platinum particle size growth is a function of many parameters, with a complex mechanism involved in Pt particle growth. However, XRD analyses of the particle size distribution provide some insight into the particle growth mechanism. The knowledge of crystallite size distribution (CSD) statistics provides important information in particle coarsening mechanisms. Ostwald ripening and coalescence mechanisms produce very different CSDs [8].

A sample platinum particle size distribution for a fresh catalyst is shown in Fig. 10a. Curve (i) is the particle distribution, (ii) the theoretical log normal distribution, (iii) is the sample log normal distribution and (iv) the cumulative distribution. As shown in Fig. 10a, the initial catalyst has a narrower particle distribution than that of the log normal; a log normal particle size distribution is common for these types of catalysts [8]. As a fuel cell MEA is operated, cathode particle size growth is observed. Fig. 10b shows the particle size distribution after fuel cell testing at a constant potential of 0.6 V for 3500 h, $T_{cell} = 80\,^{\circ}C$, with an over-saturated anode ($T_{humidifier} = 105\,^{\circ}C$) and saturated cathode humidification ($T_{humidifier} = 80\,^{\circ}C$). The cathode platinum particle size increases, along with an increase in the distribution (see Fig. 10b), but has nearly the same log normal distribution. However, during potential cycling to 1.0 V, the particle size distribution increases further to the point where the particles show essentially a theoretical log normal particle size distribution (Fig. 10c). This is an indication that the growth mechanism does not occur by long-range (via solution transport of Pt ions) Ostwald ripening. Long-range Ostwald ripening should show a particle size distribution substantially different than log normal, with a small distribution of small particles and large distribution of particles at a large particle size [2]. However, short range (particle-to-particle diffusion of Pt atoms) Ostwald ripening of

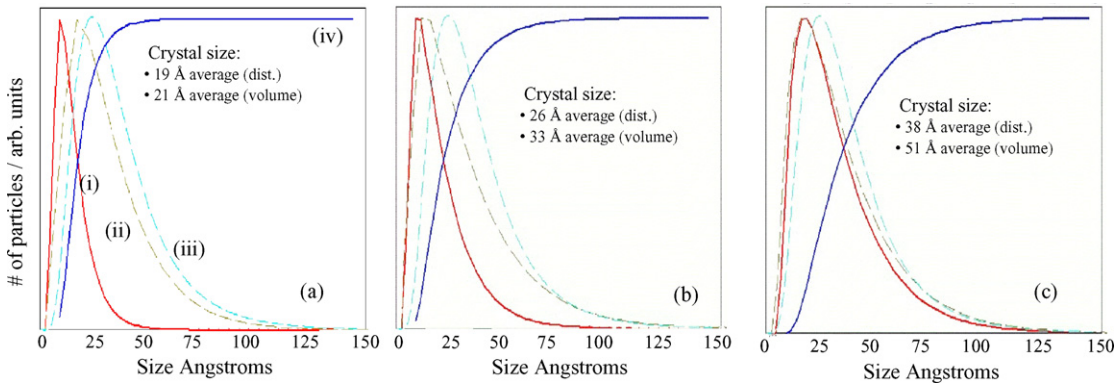

Fig. 10. Electrocatalyst particle size distribution measured by XRD (a) fresh 20 wt.% Pt catalyst, (b) testing for 3500 h at 0.6 V and (c) potential cycling to 1.0 V. Curves display: (i) particle size distribution, (ii) theoretical log normal, (iii) sample log normal and (iv) cumulative distribution.

agglomerated clusters may be occurring on relatively short time scales [8].

Measurements on platinum solubility provide additional evidence on the growth mechanism for platinum particles. Platinum solubility is a function of potential, with the Pt solubility changing increasing two orders of magnitude from potentials of 0.7 to 1.0 V [9]. Thus as a fuel cell is tested during cycling conditions (especially between ~0.7 V to open circuit (~0.96 V)), and the equilibrium platinum solubility is attained, platinum will solubilize at the high potential of open circuit, then precipitate out of solution as the potential is decreased. This agrees with the experimental observation that the route of Pt growth occurs because of the potential cycling and not due to the time at potential-time has a secondary effect compared with the number of cycles.

TEM images of the catalyst materials before and after testing [10] also give an indication of platinum particle growth mechanisms. TEM images of MEAs before testing indicate that many platinum particles are not sufficiently anchored to the carbon support, and move into the ionomer portion of the catalyst layer. During cycling measurements, these particles seem to show a more rapid tendency to coalesce into larger particles, which does not require Pt dissolution and re-precipitation. Coalescence is likely due to platinum particles increased mobility because of the lack of bonding between the platinum and carbon support. The lower growth of platinum particles at low relative humidity agrees qualitatively with both platinum solubility and particle mobility in the ionomer layer.

Our results indicate there is essentially no change in anode Pt particle size, during constant voltage, constant current, during the simulated drive cycle testing and during the off-line cycling measurements. However, we have observed reduction in the electrochemical active Pt surface area of the anode during the extended fuel cell testing (~3500 h). As the particle size of the anode did not grow (as measured by XRD), the measurement of the reduced surface area could be due to a number of factors, including loss of ionomer in the catalyst layer, Pt particle detachment from the carbon support, Pt particle mobility or an artifact of measuring the surface area in situ after long periods of testing, as these membranes typically have higher gas cross-over and can develop pin-holes.

5. Conclusions

Electrode material durability is an important factor in limiting the commercialization of polymer electrolyte membrane fuel cells (PEMFCs). We examined the loss of active catalyst surface area during fuel cell testing and developed off-line potential cycling accelerated testing. The electrochemical active catalyst surface was measure in situ by hydrogen adsorption, and the catalyst particle size was measured by X-ray diffraction.

- Electrocatalyst surface area loss is due to the growth in platinum particle size.
- Pt particle size growth is accelerated by potential cycling whether due to induced artificial cycling or by cycling such as during testing utilizing an automotive drive cycle.
- Pt particle size growth occurs more rapidly during cycling to high potentials.
- The Pt particle size rate of growth increases with increasing temperature.
- The rate of Pt particle growth decreases with decreasing relative humidity.
- Carbon corrosion was observed to increase with increasing potential and decreasing relative humidity.

Acknowledgments

This work was supported by the U.S. Department of Energy, Office of Hydrogen, Fuel Cells and Infrastructure Technology. TEM analysis was carried out by Karren More of Oak Ridge National Laboratory.

References

[1] M.S. Wilson, F.H. Garzon, K.E. Sickafus, S. Gottesfeld, J. Electrochem. Soc. 140 (10) (1993) 2872–2877.
[2] Ascarelli, Contini, Giorgi, J. Appl. Phys. 91 (7) (2002).
[3] P. Meyers, R.M. Darling, Abstract 1212, The Electrochemical Society Meeting Abstracts, vol. 2003-1, Paris, France, 2003.
[4] R. Borup, M. Inbody, J. Davey, D. Wood, F. Garzon, J. Tafoya, J. Xie and S. Pacheco, PEM Fuel Cell Durability, DOE Hydrogen Program, FY, Progress Report, 2004.

[5] M.S. Wilson, S. Gottesfeld, J. Appl. Electrochem. 22 (1992) 1.
[6] M.S. Wilson, S. Gottesfeld, J. Electrochem. Soc. 139 (1992) L28.
[7] T. Markel, National Renewable Energy Laboratory, private communication.
[8] R.A. Buhrman, C.G. Granqvist, J. Appl. Phys. 47 (5) (1976) 2220.
[9] X. Wang, R. Kumar, D. Myers, Cathode electrocatalysis: platinum stability and non-platinum catalysts, 2005 DOE Hydrogen Program Review, Arlington Va, May 25, 2005.
[10] K.L. More, K.S. Reeves, Microstructural characterization of PEM fuel cell MEAs, 2005 DOE Hydrogen Program Review, Arlington Va, May 25, 2005.